Lasers in Manufacturing Conference 2017

Distance controlled laser ablation of CFRP

Steffen Boley[a,*], Daniel Holder[a], Volkher Onuseit[a], Thomas Graf[a], Matthias Buser[a], Martin Schönleber[b]

[a] *Institut für Strahlwerkzeuge Universität Stuttgart, Pfaffenwaldring 43, Stuttgart 70569, Germany*
[b] *Precitec Optronik GmbH, Schleussnerstraße 54, Neu-Isenburg 63263, Germany*

Abstract

Precise ablation of CFRP (carbon fiber reinforced plastic) is difficult due to the highly different thermo – optical properties of fibers and plastics in combination with possible inhomogeneous parts of the material. This leads to deviations in terms of surface roughness and actual removed depth during processing. In particular, for repairing expensive parts, precise layer ablation and a certain roughness are the key points to achieve a high strength of the repaired parts.

In this approach, optical coherence tomography was combined with a galvanometer scanner. With this setup, the local depth during ablation can be measured with a spatial resolution of 5 µm and temporal resolution of 14 µs. This allows to remove material until the target depth is reached. The ablation track of the next pass is calculated by the previously measured data. As input data for the target ablation geometry, a grey-scaled bitmap picture can be used to produce any kind of 3D surface structure. The experimental validation of this setup was done with a ns laser with an average power of 20 W and a wavelength of 1047 nm. Each processing pass has an ablation depth of approximately 10 – 25 µm. Thereby a defined ablation layer by layer of CFRP part is possible. To reach the target depth of one layer, multiple passes are necessary. The ablation stops at each area when the target depth has reached. The areas are calculated by slicing the measured surface into constant depth segments. The beam passes only the segments that needs to be removed.

On the final processed area, the depth deviation was reduced to 20 µm and the roughness was reduced to below 10 µm independently from the total depth.

Keywords: Micro Processing, System Technology and Process Control, CFRP, controlled ablation;

---

* Corresponding author. Tel.: +49-771 685-66823 ; fax:-.
E-mail address: steffen.boley@ifsw.uni-stuttgart.de.

1. Introduction

Carbon Fiber Reinforced Plastic (CFRP) is made of layers of fibers of different orientation in combination with the matrix material. This structure ensures highest strength and rigidity in fiber direction, but causes problems using a laser ablation process. Therefore the production of high quality surfaces with a roughness below 60 µm with pulsed laser is challenging.

The process to repair CFRP parts damaged by an impact is to remove the damaged zone and the area around and to replace them with new material. To achieve a high strength after the reparation a high precision removal of each layer of the material is necessary as shown in Fig. 1 . The geometry of the removed area depends on the damaged zone and the lay-up of the layers can have arbitrary shapes as shown in Fig. 2.

Laser ablation of CFRP is highly influenced by the local composition of the material. The ablation rate depends mainly on the local fiber content. This leads especially for multi-layer ablation to a high roughness of the resulting surface. Without distance control, a deviation of up to 10 % was achieved. To avoid this deviation and to lower the resulting roughness an active measurement and control system is necessary. For this an optical distance-measuring device (PRECITEC CHRocodile 2) was used to scan the surface without contact. With that distance information, the parts of the scan area, which need to be ablated, can be calculated from a comparison of the measured to the desired geometry. With this information, only the necessary parts of the scan area are ablated in a second step.

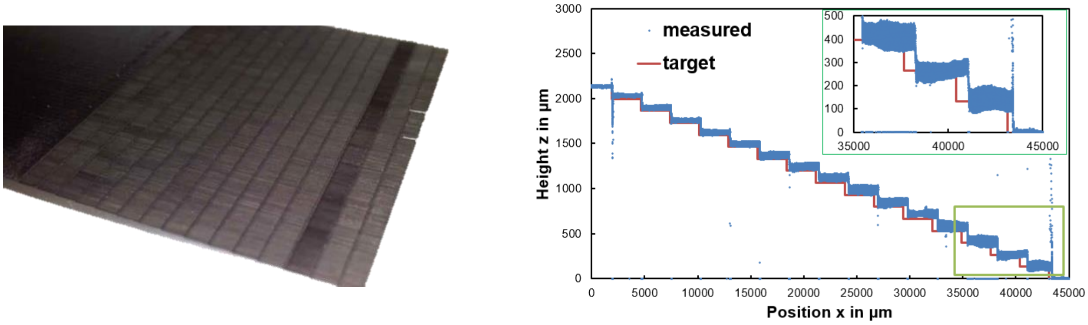

Fig. 1. Stepwise ablation of CFRP with linear steps.

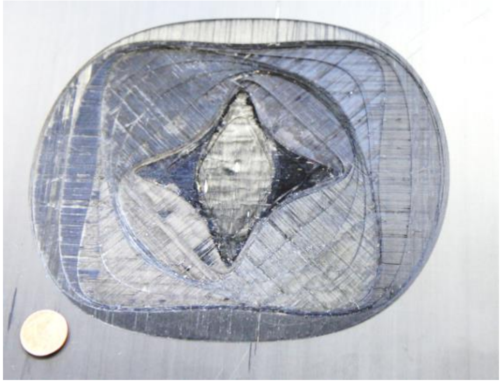

Fig. 2. Stepwise ablation of CFRP with optimized shape of the ablation area.

2. Ablation Strategy

With the developed setup, different types of a controlled ablation strategy can be compared to the conventional uncontrolled ablation. First, the sequential controlled ablation as a two step process with sequential runs for measurement and ablation and the simultaneous ablation with measurement and ablation in one scan.

2.1. Conventional ablation

The uncontrolled conventional ablation, with fixed count of passes, is state of the art, shown by Weber et al. 2011. The processing beam hatches the sample with a predefined count of passes. The number of scans is derived from an experimental determined ablation rate to achieve the needed ablation depth. In this case different local material properties lead to low quality surfaces.

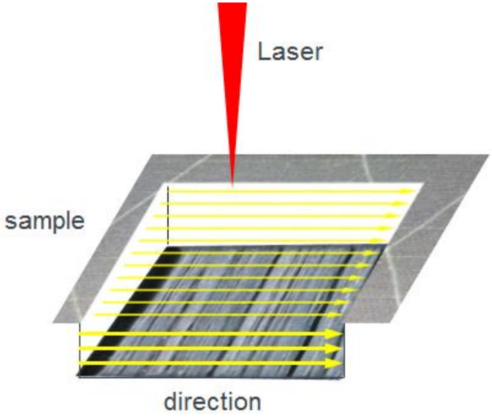

Fig. 3. Conventional ablation with parallel hatching

2.2. Sequential controlled ablation

A scheme of the controlled ablation with sequential processing and measuring is shown in Fig. 4. The so-called “pixel mode” of the galvo scanner passes each hatching line with a predefined power list. The ablation pass has the same hatching strategy as the conventional process, but the Laser is only on in the necessary areas, preset by a pixel map. After each ablation pass, an extra measuring pass is done. Based on the measuring data, a depth map is calculated and compared to the target depth. If the depth has not reached the target value, the cycle starts again. This procedure is repeated until the whole area (up to 98 %) has reached the target depth.

The measuring is done with a higher speed of 3.5 m/s than the ablation. Due to this the measuring pass is 6 times faster than the ablation and the total processing time is only increased by 16% in comparison to the conventional strategy.

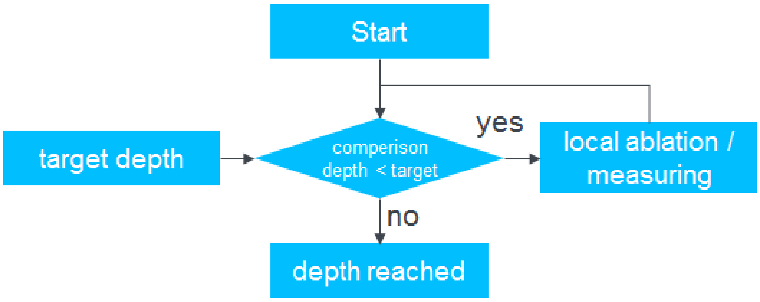

Fig. 4. Scheme of sequential controlled ablation

2.3. *Simultaneous ablation and measuring*

In comparison to the strategy described before, the measuring and the ablation is done in one pass and there is no increase of the overall processing time.

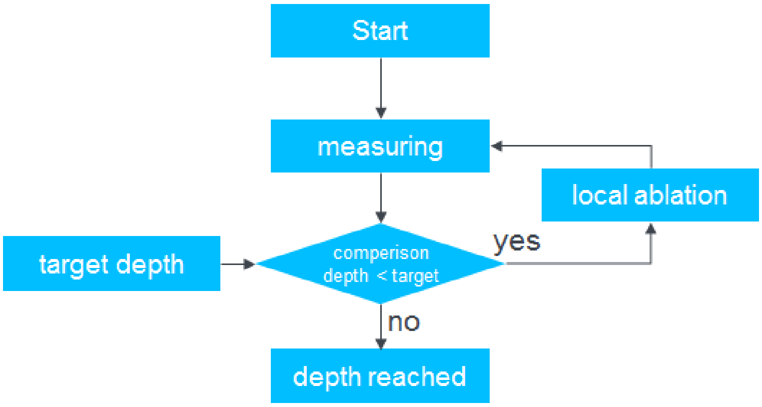

Fig. 5. Scheme of simultaneous controlled ablation

3. Experimental Setup

The experiments were carried out with a combined galvanometer scanner and an optical distance-measuring device as shown in Fig. 6. A dichroitic mirror combines the processing-beam (wavelength 1047 nm) and the measuring-beam (wavelength 1060 - 1100 nm). Both are passing the galvanometer scanner as well as the f-theta-lens and are focused on the sample. The beams have been adjusted to the same spot. As processing laser a ns pulsed Laser was used with an average power 16 W. Processing parameters are listed in Table 1. The measuring beam is produced by the CHRocodile2 from PRECITEC, reflected by the sample, back into the device. The measurement principle is described in Schmitt et al. 2013.

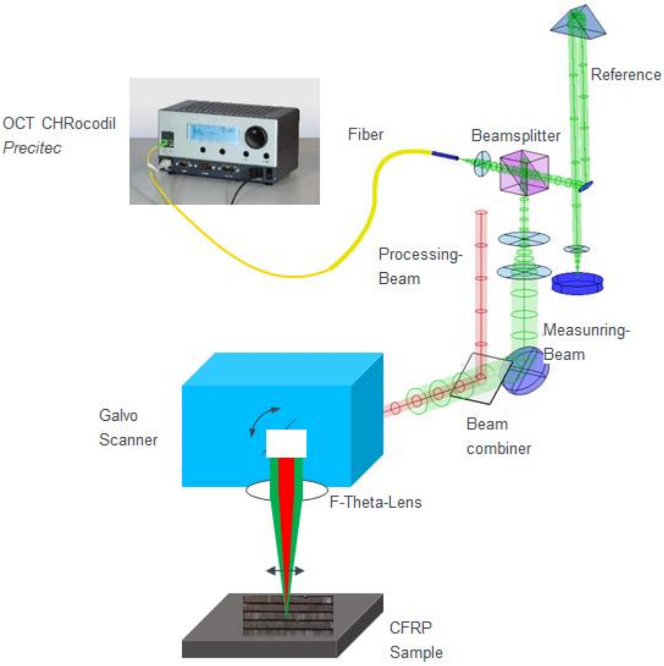

Fig. 6. Experimental setup: Distance measuring, Processing beam, Galvo-Scanner

The experimental setup for the machining is shown in
Fig. 7. To remove the ablated material the processing is carried out in a suction box showed on the left. The parameters shown in Table 1 have been used for processing.

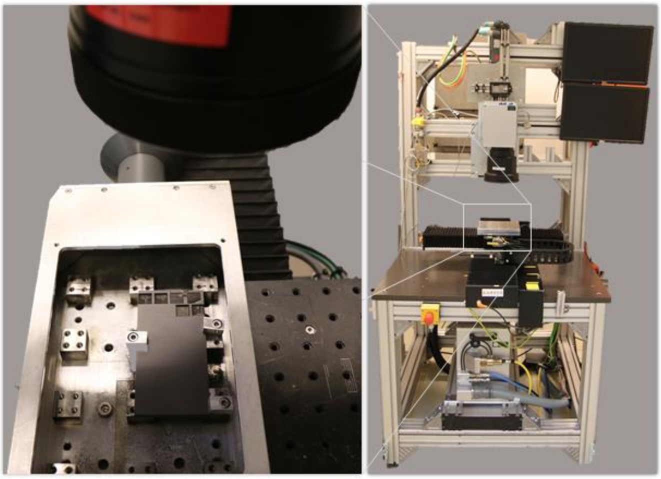

Fig. 7. Experimental setup: suction box and sample (left), processing system (right).

Table 1. Processing an measuring parameters

Laser parameters	Distance measurement CHRocodile2:	Galvanometer scanner
Pulse energy of 1,4 mJ	Power 100 mW	Feed rate 600 mm/s (36 m/min)
Repetitions rate 15 kHz	Measuring rate 70 kHz	Hatching distance 60 µm
Raw beam 5 mm	Raw beam 17 mm	Focusing lens 163 mm
Focus diameter 50 µm	Focus diameter 15 µm	
Wavelength 1047 nm	Wavelength 1060 - 1100 nm	
$M^2 < 1.3$	$M^2 < 1.1$	

For the processing, CFRP samples with unidirectional as well as multidirectional layup with a layer height 625 µm were used. Squares with size between 10 and 20 mm were ablated with a hatching distance of 60 µm. Hatching direction on all samples was from left to right. With the processing parameters shown before (1.4 mJ, 15 KHz) a high ablation rates up to 0.7 mm³/s was achieved and the size of the heat affected zone was minimized (Zahedi et al. 2015).

4. Processing Result

The result of the ablation with sequential controlled ablation and measuring is shown in Fig. 8 compared to the uncontrolled conventional processing with the same depth of 1 mm. A rough surface is visible for the conventional strategy. The inhomogeneous distribution of matrix material and its different absorption of the laser leads to grooves along the rowings. Due to this the fiber rowings are visible in vertical direction. In Fig. 9 the resulting roughness as cross section perpendicular to the fibers is shown. The conventional ablation on the left has an arithmetic average roughness S_a of about 60 µm measured concerning the ISO 25178 and a max. deviation of 200 µm. In comparison this controlled process leads to a surface roughness of S_a = 7 µm and a max. deviation of 20 µm.

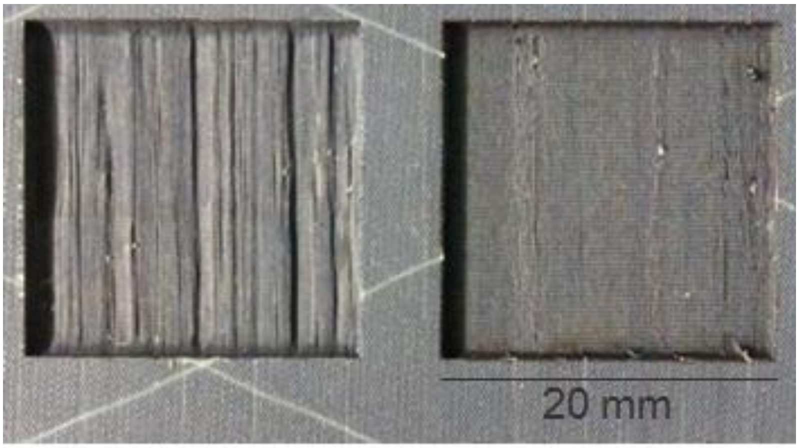

Fig. 8. Result: Uncontrolled ablation (left), controlled ablation (right), for unidirectional fibers.

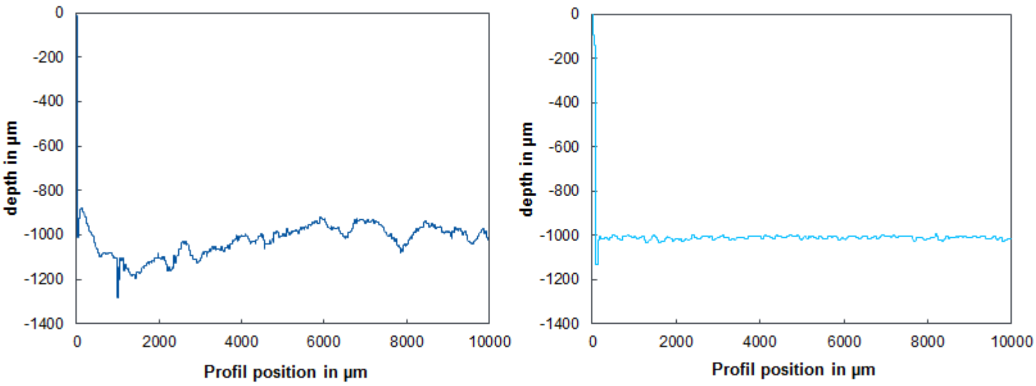

Fig. 9. Cross section: Uncontrolled ablation (left), controlled ablation (right).

Fig. 10 shows the result for a controlled ablation of a step geometry with a constant layer height of 0.3 mm. The deviation of a single step from the expected depth is below 10 µm. Compared to Fig. 2 the layers are clearly visible with constant height. In Fig. 11 the evolution of the geometry is shown with measured data after each processing step. Deep red is the surface (0 mm) deep green (1.5 mm) is the lowest layer. The first four passes ablate the first layer. From pass 5 until 12, the stepwise ablation takes place. The last 12 passes are only for fine ablation to reduce the roughness and the final depth of 1.5 mm. The processing laser was only switched on locally on the necessary areas.

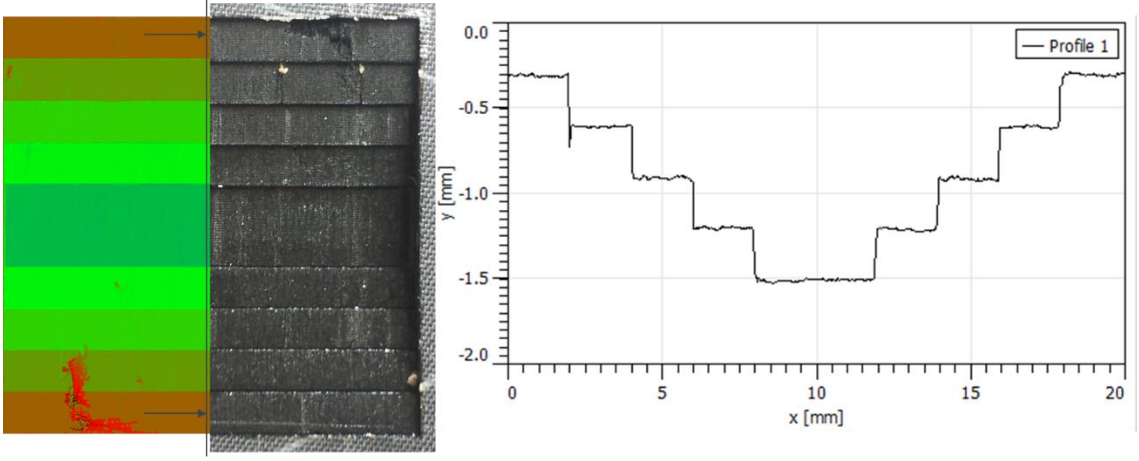

Fig. 10. Cross section of stepwise controlled ablation after the final pass.

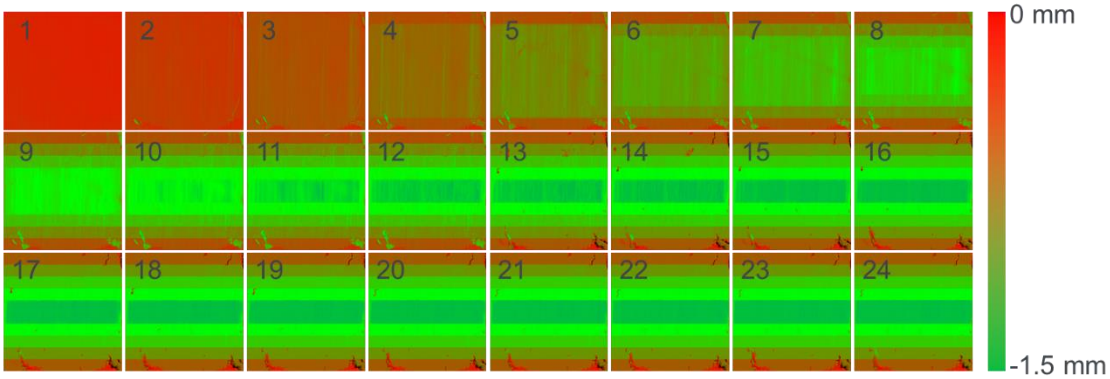

Fig. 11. Measuring data, after controlled processing of stepwise ablation.

For demonstration purpose, the toolchain from CAD (Computer Aided Design) files, over CAM (Computer Aided Manufacturing) to the real part can also be reduced with the controlled ablation. A sample part as shown in Fig. 12 can be produced without any programming effort. It consists of different geometries to show the full freeform design ability. On the left, the constructed CAD file as well as a converted grey-scaled picture is shown. This picture was taken as input file for the ablation software. The right side shows the final part as a false colour measured height map as well as a picture of the real sample. The white dots are plastic fibers inside the material from the production of the fiber layers. The absorption of the matrix (epoxy resin) as well as these plastic fibers is lower (< 1 %) than the absorption of the carbon fibers (shown by Bismarck et al., 2016). This leads to small plastic fiber parts on the surface which have to be removed manually.

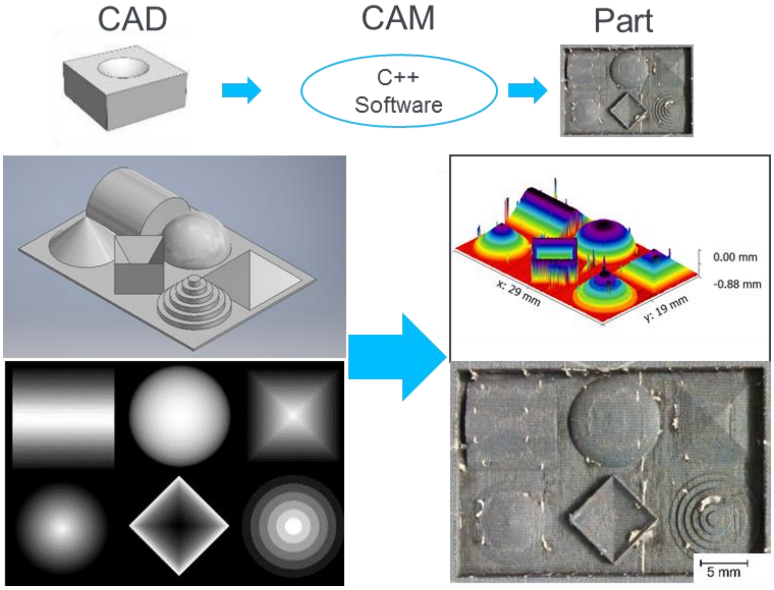

Fig. 12. Toolchain from CAD file to the real part.

5. Conclusion

This work showed the benefits of a controlled ablation strategy. A pulsed laser system in combination with a galvanometer and a fast optical distance measurement system was used. This improved the quality of ablated CFRP surfaces drastically and lead to a reduction of the roughness from 60 to 7 µm and the deviation from 200 to 20 µm compared to a non-controlled process. A full toolchain was shown and offers the ability to process individual CFRP parts. Without knowledge about its layer composition and independent from variating ablation rates, step geometries as well as designed freeform surfaces were produced.

Further tests will be done with higher power processing laser to get higher ablation rates. This will improve the productivity as well as the field of applications. A few optimizations steps in the software and the strategy will reduce the overall processing time as well.

Acknowledgements

The authors acknowledge the financing of this work by the Bundesministerium für Bildung und Forschung (BMBF) in the frame of the project PRECISE under Contract No. 13N12922.

References

Bismarck, A., Blaker, J. J., Anthony, D. B., Qian, H., Maples, H. A., Robinson, P. et al. (2016) Development of novel composites through fibre and interface/interphase modification. In : IOP Conference Series: Materials Science and Engineering, vol. 139, p. 12001. DOI: 10.1088/1757-899X/139/1/012001.

Leung, Ben Y. C., Webster, Paul J. L., Fraser, James M., Yang, Victor X. D. (2012) Real-time guidance of thermal and ultrashort pulsed laser ablation in hard tissue using inline coherent imaging. In : Lasers in surgery and medicine, vol. 44, n° 3, p. 249–256. DOI: 10.1002/lsm.21162}.

Neef, A., Seyda, V., Herzog, D., Emmelmann, C., Schönleber, M., Kogel-Hollacher, M. (2014) Low Coherence Interferometry in Selective Laser Melting. In : Physics Procedia, vol. 56, p. 82–89. DOI: 10.1016/j.phpro.2014.08.100.

Schmitt, R., Mallmann, G., Winands, K., Pothen, M. (2013) Automated Process Initialization of Laser Surface Structuring Processes by Inline Process Metrology. In : Physics Procedia, vol. 41, p. 887–895. DOI: 10.1016/j.phpro.2013.03.163.

Weber, R., Hafner, M., Michalowski, A., and Graf, T. (2011) Minimum damage in CFRP laser processing, in Proceedings of the Sixth International Wlt Conference on Lasers in Manufacturing, Munich, Germany, 302-307.

Zahedi, E., Freitag, C., Wiedenmann, M., Onuseit, V., Weber, R., Graf, T. (2015) High ablation rate laser processing of CFRP for repair purpose, in Proceedings of ICALEO, Sheraton Atlanta, USA, M304.